

# Calmodulin Kinase II Interacts with the Dopamine Transporter C Terminus to Regulate Amphetamine-Induced Reverse Transport

Jacob U. Fog,<sup>1,2,8</sup> Habibeh Khoshbouei,<sup>3,8</sup>  
Marion Holy,<sup>5</sup> William A. Owens,<sup>6</sup>  
Christian Bjerggaard Vaegter,<sup>1</sup> Namita Sen,<sup>7</sup>  
Yelyzaveta Nikandrova,<sup>3</sup> Erica Bowton,<sup>3</sup>  
Douglas G. McMahon,<sup>4</sup> Roger J. Colbran,<sup>3</sup>  
Lynette C. Daws,<sup>6</sup> Harald H. Sitte,<sup>5</sup>  
Jonathan A. Javitch,<sup>7,9</sup> Aurelio Galli,<sup>3,9</sup>  
and Ulrik Gether<sup>1,9,\*</sup>

<sup>1</sup>Molecular Neuropharmacology Group and  
Center for Pharmacogenomics  
Department of Pharmacology  
The Panum Institute  
University of Copenhagen  
DK-2200 Copenhagen  
Denmark

<sup>2</sup>H. Lundbeck A/S  
DK-2500 Valby  
Denmark

<sup>3</sup>Department of Molecular Physiology  
and Biophysics and  
Center for Molecular Neuroscience

<sup>4</sup>Department of Biological Science  
Vanderbilt University School of Medicine, Nashville  
Nashville, Tennessee 37232

<sup>5</sup>Center for Biomolecular Medicine and Pharmacology  
Institute of Pharmacology  
Medical University Vienna  
Waehringerstrasse 13a, A-1090 Vienna  
Austria

<sup>6</sup>Department of Physiology  
University of Texas Health Science Center  
at San Antonio  
San Antonio, Texas 78229

<sup>7</sup>Center for Molecular Recognition and the  
Departments of Psychiatry and Pharmacology  
Columbia University College of  
Physicians & Surgeons  
630 West 168th Street, P&S 11-401  
New York, New York 10032

## Summary

Efflux of dopamine through the dopamine transporter (DAT) is critical for the psychostimulatory properties of amphetamines, but the underlying mechanism is unclear. Here we show that Ca<sup>2+</sup>/calmodulin-dependent protein kinase II (CaMKII) plays a key role in this efflux. CaMKII $\alpha$  bound to the distal C terminus of DAT and colocalized with DAT in dopaminergic neurons. CaMKII $\alpha$  stimulated dopamine efflux via DAT in response to amphetamine in heterologous cells and in dopaminergic neurons. CaMKII $\alpha$  phosphorylated serines in the distal N terminus of DAT in vitro, and mutation of these serines eliminated the stimulatory

effects of CaMKII $\alpha$ . A mutation of the DAT C terminus impairing CaMKII $\alpha$  binding also impaired amphetamine-induced dopamine efflux. An in vivo role for CaMKII was supported by chronoamperometry measurements showing reduced amphetamine-induced dopamine efflux in response to the CaMKII inhibitor KN93. Our data suggest that CaMKII $\alpha$  binding to the DAT C terminus facilitates phosphorylation of the DAT N terminus and mediates amphetamine-induced dopamine efflux.

## Introduction

Abuse of amphetamines (AMPHs) represents a major societal problem with more than 35 million methamphetamine abusers worldwide. The consequences of methamphetamine use are severe and include dependence, overdose, and death (Rawson et al., 2002). AMPHs and other psychostimulants also can induce psychosis and paranoia in normal subjects, and patients with schizophrenia show increased sensitivity to the psychotogenic effects of these compounds (Lieberman et al., 1997). Nonetheless, the molecular mechanisms underlying the effects of AMPHs on the human brain and how they might lead to addiction are still poorly understood.

The principal target for the action of AMPHs is believed to be the dopamine transporter (DAT), which belongs to the solute carrier 6 (SLC6) gene family of Na<sup>+</sup>/Cl<sup>-</sup>-coupled transporters that also includes the transporters for other neurotransmitters such as norepinephrine, serotonin, glycine, and GABA (Amara and Kuhar, 1993; Chen et al., 2004; Torres et al., 2003). The DAT controls dopaminergic signaling by mediating rapid reuptake of dopamine (DA) from the synaptic cleft. In addition to AMPHs, other psychostimulants, including cocaine, also target the DAT (Amara and Kuhar, 1993; Chen et al., 2004; Torres et al., 2003). Cocaine acts as a simple inhibitor that binds to the DAT and blocks transport activity. In contrast, AMPHs are substrates that are actively transported (Sitte et al., 1998; Sulzer et al., 2005; Wall et al., 1995). As substrates, AMPHs not only competitively inhibit DA reuptake and thereby increase synaptic DA but also promote reversal of transport, resulting in efflux of DA via the DAT (Sulzer et al., 2005). This efflux results in a dramatic increase in extracellular dopamine and is believed to be of major importance for the psychostimulatory properties of AMPHs (Sulzer et al., 2005). The mechanism by which AMPHs elicit the efflux is nonetheless unclear.

The DAT is hypothesized to function via an alternate access mechanism in which binding of substrate together with Na<sup>+</sup> and Cl<sup>-</sup> triggers a conformational change that leads to transition of the transporter from an “outward-facing” conformation, in which the substrate binding site is exposed to the extracellular milieu, to an “inward-facing” conformation, in which the substrate binding site is exposed to the intracellular milieu (Jardetzky, 1966; Loland et al., 2003). According to this scheme, efflux has been suggested to occur via a facilitated exchange mechanism, i.e., the transport of AMPH

\*Correspondence: gether@neuropharm.ku.dk

<sup>8</sup>These authors contributed equally to this work.

<sup>9</sup>These authors contributed equally to this work.

into the cell would increase the number of transporters in the inward-facing conformation and in this way increase the likelihood that DA is transported out of the cells by exchange (Fischer and Cho, 1979). However, increasing evidence has challenged this model and suggested that AMPH-induced DA efflux is not directly coupled to uptake (Pifl and Singer, 1999; Scholze et al., 2002) and might even involve a channel-like mode of the transporter (Kahlig et al., 2005; Sitte et al., 1998). The DA efflux induced by AMPH also appears to rely on an increase in both intracellular sodium and calcium (Gnegy et al., 2004; Khoshbouei et al., 2003). Moreover, we have demonstrated that phosphorylation of serines in the distal N terminus of DAT mediates the ability of AMPHs to promote DA efflux by shifting the transporter from a “reluctant” to a “willing” state for efflux without interfering with inward transport (Khoshbouei et al., 2004). Although AMPH-induced DA efflux is regulated by certain protein kinase C isoforms, especially the  $\beta$  isoform (Gnegy, 2003; Johnson et al., 2005), other kinases might also be involved (Kantor et al., 1999; Pierce and Kalivas, 1997).

Here we provide evidence that  $\text{Ca}^{2+}$ /calmodulin-dependent protein kinase  $\alpha$  (CaMKII $\alpha$ ) plays a key role in mediating the ability of AMPH to efflux DA through DAT. Using the C terminus of the human DAT as bait, we identify in a yeast two-hybrid screen CaMKII $\alpha$  as a direct interaction partner of DAT. The interaction with the DAT C terminus is confirmed in GST fusion pull-down experiments and by coimmunoprecipitations, and DAT is shown to colocalize with CaMKII $\alpha$  in mid-brain dopaminergic neurons. We also provide evidence from *in vitro* and *in vivo* experiments that the association of CaMKII $\alpha$  with the DAT C terminus facilitates phosphorylation of N-terminal serines, which in turn supports reversal of transport and thereby DA efflux.

## Results

### CaMKII $\alpha$ Associates with the DAT C Terminus

In a yeast two-hybrid screen using the C terminus of the human DAT as bait against a human brain cDNA library, we identified a clone (clone 2-36) that encoded an in-frame fusion with the association domain of CaMKII $\alpha$  (Figure 1A). This C-terminal domain is involved in oligomerization of CaMKII $\alpha$  and mediates interaction with other proteins, including densin-180 (Robison et al., 2005; Strack et al., 2000; Walikonis et al., 2001). The interaction between CaMKII $\alpha$  and the DAT C terminus was validated using purified CaMKII $\alpha$  autophosphorylated with [ $\gamma$ - $^{32}\text{P}$ ]ATP in the presence of  $\text{Ca}^{2+}$  and calmodulin (CaM). C-terminal glutathione-S-transferase (GST) fusion proteins containing either the last 46 C-terminal residues (C46) or the last 24 residues (C24) of DAT were capable of pulling down the  $^{32}\text{P}$ -labeled kinase, [ $^{32}\text{P}$ -Thr286]CaMKII $\alpha$  (Figures 1B and 1C). In contrast, GST itself and a fusion protein encoding the N terminus of DAT (amino acids 1–69) did not bind [ $^{32}\text{P}$ -Thr286]CaMKII $\alpha$  (Figure 1D). Like C24 and C46, a C-terminal fusion encoding the 40 C-terminal residues (C40) of DAT was capable of pulling down [ $^{32}\text{P}$ -Thr286]CaMKII $\alpha$ , but deleting the 11 C-terminal residues of this fusion protein (C40del11) markedly reduced binding (Figures 1D and 1G). In contrast to the results for DAT fusion proteins, a GST fusion protein containing the last 24 residues of the homolo-

gous norepinephrine transporter (NET) pulled down CaMKII $\alpha$  only very inefficiently and not to a significant extent (Figures 1E and 1G), whereas the corresponding serotonin transporter (SERT) GST fusion protein failed to pull down CaMKII $\alpha$  (Figures 1E and 1G).

To further explore the structural requirements for CaMKII $\alpha$  binding, we performed a series of triple-alanine substitutions in the C24 fusion protein (Figures 1E and 1F). Substitution to alanine of 612–614 and 615–617 caused a marked decrease in binding of [ $^{32}\text{P}$ -Thr286]CaMKII $\alpha$  (Figures 1E and 1F). The lack of binding was not due to degradation or lower concentration of the GST fusion proteins, since staining the gel for protein revealed GST fusion protein bands of similar intensity and size (data not shown). Regardless of their ability to bind CaMKII $\alpha$ , both 612–14 and 615–17, as well as 606–08 and 609–11, were still capable of pulling down protein interacting with C kinase-1 (PICK-1) (see Figure S1 in the Supplemental Data available online), another protein known to interact with the DAT and NET C termini (Bjerggaard et al., 2004; Torres et al., 2001). We further confirmed the importance of the DAT C terminus for interaction with CaMKII $\alpha$  in GST pull-down experiments using lysates from T-Rex HEK293 cells that expressed full-length CaMKII $\alpha$  in a tetracycline-inducible manner (T-Rex HEK293 CaMKII $\alpha$ ) (Figure 2A). Pull-down experiments using rat brain homogenates also showed that the DAT C terminus can bind endogenously expressed CaMKII $\alpha$  (Figure 2B).

We assessed next whether CaMKII $\alpha$  and DAT interact in a cellular environment by coimmunoprecipitation experiments using T-Rex HEK293 CaMKII $\alpha$  cells that were transfected with DAT. CaMKII $\alpha$  was present in immunoprecipitates obtained with an anti-DAT antibody from DAT-transfected cells but not from nontransfected control cells (Figure 2C). CaMKII $\alpha$  also was not present in control precipitates obtained in the absence of antibody (Figure 2C) or with a control antibody (data not shown). Conversely, DAT was present in immunoprecipitates obtained with a CaMKII $\alpha$ -specific antibody and not in control precipitates obtained without antibody (Figure 3B). These data demonstrate that DAT and CaMKII $\alpha$  can exist as a complex in living cells.

As a control and to demonstrate further that SERT does not interact with CaMKII $\alpha$ , we used T-Rex HEK293 CaMKII $\alpha$  cells transfected with either *c-myc*-tagged SERT or *c-myc*-tagged DAT (Figure S2). CaMKII $\alpha$  was present in the immunoprecipitates obtained with a mouse anti-*c-myc* antibody from the *c-myc*-hDAT-transfected cells, whereas we observed no or only a very faint band corresponding to CaMKII $\alpha$  in immunoprecipitates from the *c-myc*-hSERT-transfected cells (Figure S2). As yet another control, the CaMKII $\alpha$  antibody did not pull down a control membrane protein (FLAG-tagged  $\delta$ -opioid receptor) when it was expressed in the cells instead of DAT (data not shown).

To assess for colocalization of CaMKII $\alpha$  and DAT in neurons, we prepared postnatal cultures of rat midbrain dopaminergic neurons and visualized DAT by double staining using two different DAT antibodies (MAB369, directed against the DAT N terminus, and AB5802, directed against the second extracellular loop). As expected, the staining patterns overlapped (Figure 3). DAT immunoreactivity displayed a cluster-like pattern

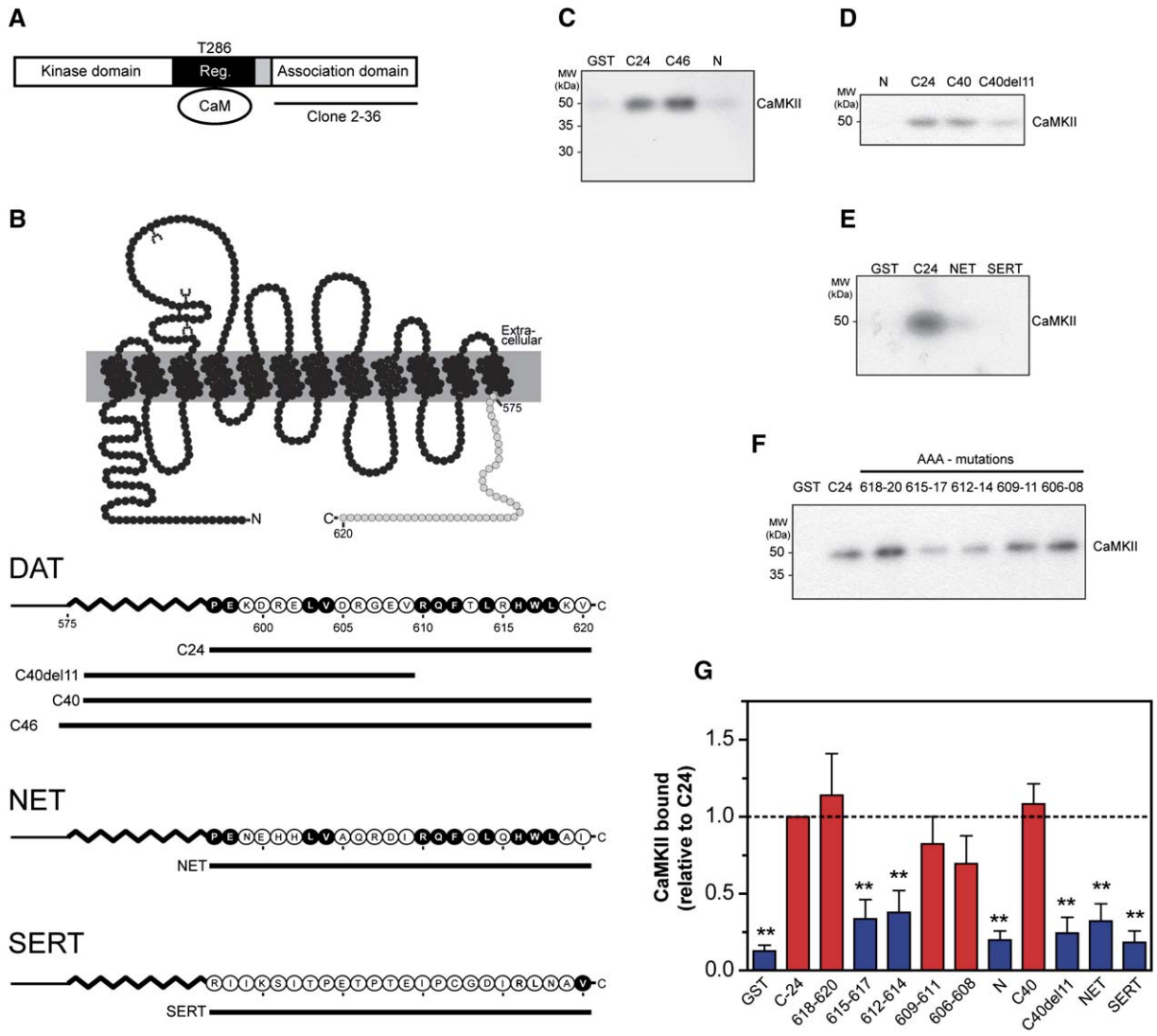


Figure 1. CaMKII $\alpha$  Interacts with the C Terminus of the Dopamine Transporter

(A) Schematic view of CaMKII $\alpha$ . The N-terminal kinase domain is activated by phosphorylation of Thr286, which is induced by Ca<sup>2+</sup>/calmodulin (CaM) association with the regulatory domain (Reg). A yeast two-hybrid screen using the C-terminal 46 residues of the human DAT as bait against a human brain cDNA library identified a clone (2–36) that was an in-frame fusion with a sequence encoding the association domain of CaMKII $\alpha$ .

(B) Diagram of the hDAT topology. The C-terminal residues marked in gray are those used for the yeast two-hybrid screen. Below is a representation of DAT, NET, and SERT GST fusion proteins used in pull-down experiments.

(C–E) Representative GST pull-down experiments of [<sup>32</sup>P]CaMKII $\alpha$  comparing (C) GST with DAT C24, C46, and the N-terminal fusion protein (N); (D) the N-terminal fusion with DAT C24, C40, and C40del11; (E) DAT C24 with the corresponding NET and SERT fusion proteins.

(F) DAT C24 with C24 containing the indicated triple Ala substitutions. In the experiments, bound [<sup>32</sup>P]CaMKII $\alpha$  was detected by SDS-PAGE followed by autoradiography of the gel.

(G) Densitometric analysis of pull-down experiments. Data are shown as binding relative to C24 (means  $\pm$  SE, n = 3–12, \*p < 0.05, \*\*p < 0.01, one-way ANOVA, Dunnett's post hoc test).

along the neuronal projections in agreement with previous observations (Figure 3) (Torres et al., 2001). Most neurons that stained for DAT (MAB369) also stained for tyrosine hydroxylase (TH) (Figure 3), and approximately 25% of the cells could be classified as dopaminergic based on this dual pattern of staining (data not shown). DAT also colocalized with the vesicular monoamine transporter 2 (VMAT2), a presynaptic protein selectively expressed in monoaminergic neurons (Figure 3). Double staining for DAT and CaMKII revealed expression of CaMKII in the neurons that expressed DAT, as well as in other neurons. In the neurons that ex-

pressed both DAT and CaMKII, we observed significant colocalization of the two proteins (Figure 3).

#### The N Terminus of DAT Is a Substrate for CaMKII $\alpha$ In Vitro

In rats repeatedly treated with intermittent AMPH or cocaine, locomotor behavior and DA efflux in response to a subsequent test dose of AMPH were increased, and this effect was blocked by an inhibitor of CaMKII (Kantor et al., 1999; Pierce and Kalivas, 1997). In addition, AMPH treatment increases CaMKII activity in striatal synaptosomes (Iwata et al., 1997). We decided accordingly to

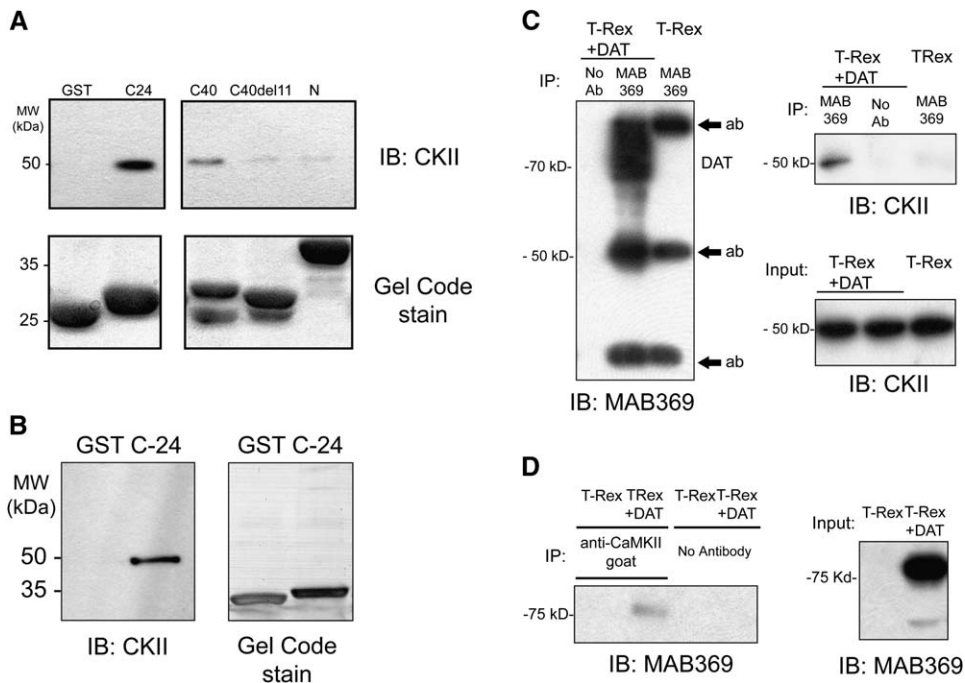


Figure 2. GST Pull-Down and Coimmunoprecipitation Experiments of CaMKII $\alpha$  with DAT

(A) (Upper panels) Representative (of  $n = 3-4$ ) GST pull-down experiment of CaMKII $\alpha$  in lysates from T-Rex HEK293 cells that expressed full-length CaMKII $\alpha$  in a tetracycline-inducible manner (T-Rex HEK293 CaMKII $\alpha$ ) comparing GST alone with GST hDAT C24, C40, C40del11, and the N-terminal hDAT GST fusion protein. Bound CaMKII $\alpha$  was detected by SDS-PAGE followed by immunoblotting. (Lower panels) GelCode Blue stain of the gel showing the different GST fusions used in the pull-down experiments. The partial degradation of GST-C40 may explain the lower intensity of the CaMKII $\alpha$  band seen on the immunoblots.

(B) Representative (of  $n = 4$ ) GST pull-down experiment of CaMKII $\alpha$  from solubilized crude rat synaptosomes comparing GST alone with GST hDAT C24. (Left panel) Immunoblot of SDS-PAGE with mouse anti-CaMKII $\alpha$  antibody showing pull down by the hDAT C terminus but not by GST alone. (Right panel) A GelCode Blue stain (Pierce) of the PVDF membrane showing equal loading of GST fusion proteins.

(C) CaMKII $\alpha$  coimmunoprecipitates with hDAT. Immunoprecipitation was performed with MAB369 anti-DAT antibody using lysates prepared from T-Rex HEK293 CaMKII $\alpha$  cells transiently expressing DAT (T-Rex + DAT) and untransfected T-Rex HEK293 CaMKII $\alpha$  (T-Rex). The immunoprecipitates were analyzed by 10% SDS-PAGE and immunoblotted with the MAB369 anti-DAT antibody (left panel). A control with no primary antibody (MAB369) was done in parallel (no Ab). Nonspecific antibody bands derived from MAB369 are indicated with arrows. Corresponding samples were analyzed in parallel and immunoblotted with goat anti-CaMKII $\alpha$  antibody (upper right panel). A band corresponding to the size of CaMKII $\alpha$  (~50 kDa) was only seen with the hDAT-expressing cells in the presence of MAB369 antibody. (Lower right panel) SDS-PAGE and immunoblotting with goat anti-CaMKII $\alpha$  antibody of the whole-cell lysates used for the immunoprecipitations.

(D) (Left panel) Immunoprecipitation with goat anti-CaMKII $\alpha$  antibody from T-Rex HEK293 CaMKII $\alpha$  cells transiently expressing hDAT (T-Rex + DAT) and untransfected T-Rex HEK293 CaMKII $\alpha$  cells (T-Rex). The immunoprecipitates were analyzed by 10% SDS-PAGE and immunoblotted with the MAB369 anti-DAT antibody. A control with no primary antibody was done in parallel (no Ab). A band eluting corresponding to the size of hDAT (~75 kDa) was only seen in the hDAT-expressing cells. (Right panel) SDS-PAGE and immunoblotting with MAB369 anti-DAT antibody of the whole-cell lysates used for the immunoprecipitations. The immunoprecipitations shown are representative of three to five experiments with similar results.

investigate the involvement of CaMKII in AMPH-induced DA efflux and to assess the functional role of CaMKII association with the DAT C terminus. Since we recently showed that phosphorylation of DAT N-terminal serines is critical for AMPH-induced DA efflux (Khoshbouei et al., 2004), we first wanted to assess whether CaMKII could phosphorylate these serines. Notably, none of the serines in the N terminus of DAT are within a classical consensus sequence for any known kinase, and the N-terminal serine(s) in DAT that is (are) phosphorylated is unknown. We tested the ability of a series of protein kinases to incorporate phosphate into a peptide corresponding to the first 27 residues of hDAT. Phosphorylation of the N-terminal peptide was compared with that of appropriate control substrates for each kinase (see Experimental Procedures). The efficiency of CaMKII $\alpha$  phosphorylation of the hDAT peptide was ~31% of

that of the control substrate, autocalmitide 2 (Figure 4). In comparison, PKC $\alpha$  phosphorylated the peptide with an efficiency of ~42% as compared to the control substrate histone (Figure 4). In contrast, none of the other kinases tested incorporated significant phosphate into the N-terminal peptide (Figure 4). Thus, at least in vitro, serines in the DAT N terminus are substrates for both CaMKII $\alpha$  and PKC $\alpha$ .

#### Activated CaMKII $\alpha$ Stimulates AMPH-Induced DAT-Mediated DA Efflux

To assess directly the role of CaMKII in AMPH-induced DAT-mediated DA efflux, we combined amperometry with the patch-clamp technique in the whole-cell configuration (Khoshbouei et al., 2004). This allowed recording of DAT-mediated currents while simultaneously measuring DA efflux by amperometry (Khoshbouei

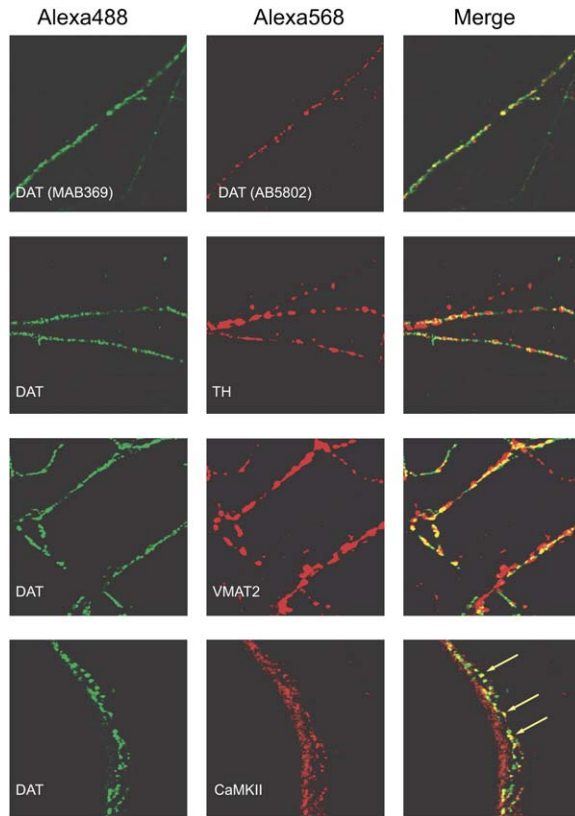


Figure 3. Colocalization of DAT and CaMKII $\alpha$  in Midbrain Dopaminergic Neurons

The neurons were fixed in 4% paraformaldehyde, permeabilized and stained with (upper panel) two different anti-DAT antibodies (MAB369, directed against the DAT N terminus, and AB5802, directed against the second extracellular loop), (upper middle panel) the anti-DAT MAB369 antibody and an anti-tyrosine hydroxylase (TH) antibody, (lower middle panel) the anti-DAT MAB369 antibody and an anti-VMAT2 antibody, or (lower panel) the anti-DAT MAB369 antibody and an anti-CaMKII antibody. For secondary antibodies we used goat anti-rat Alexa Fluor 488 (1:1000) and goat anti-rabbit Alexa Fluor 568 (Molecular Probes). Arrows indicate specific points of colocalization of CaMKII and DAT. Stained cells were visualized using a Zeiss LSM 510 confocal laser scanning microscope with an oil-immersion 63 $\times$  objective using a 505–530 nm bandpass filter for Alexa Fluor 488 fluorescence and 585 nm long-pass filter for Alexa Fluor 568 fluorescence.

et al., 2004). With the whole-cell pipette we could also perfuse the intracellular environment with purified CaMKII $\alpha$ . Addition of the activated kinase to the patch pipette caused a significant increase in the voltage-dependent AMPH-induced DA efflux (Figure 5A, left panels) as well as in the associated whole-cell current (Figure 5A, right panels). At +100 mV, the efflux of DA was approximately doubled as compared to that seen upon addition of heat-inactivated CaMKII $\alpha$  to the pipette (Figure 5A, left panels). Representative traces are shown in the upper panels, whereas the corresponding current-voltage relationships for the amperometric and whole currents are shown in the lower panels of Figure 5A. This CaMKII $\alpha$  regulation did not result from changes in the electrochemical gradient, since no change in the reversal potential of the AMPH-induced whole-cell current was observed (Figure 5A, lower panels). To test whether the stimulatory effect of CaMKII $\alpha$  was dependent on

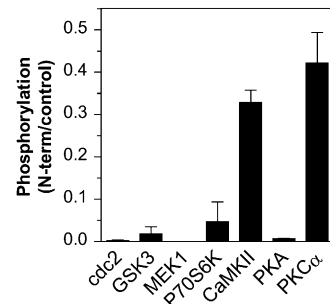


Figure 4. CaMKII $\alpha$  Phosphorylates the DAT N Terminus In Vitro

The relative phosphorylation efficiency of an N-terminal DAT peptide (residues 1–27) is shown for seven different kinases as described in Experimental Procedures. The data are expressed as phosphorylation relative to a standard substrate peptide (autocamtide 2 and histone H1, for CaMKII $\alpha$  and PKC $\alpha$ , respectively) (means  $\pm$  SD). The experiments were performed in triplicate and repeated twice. Under the initial rate conditions of the assay,  $2.0 \pm 2.0$ ,  $3.5 \pm 3.2$ ,  $1.5 \pm 0.8$ ,  $3.2 \pm 3.2$ ,  $31.5 \pm 2.8$ ,  $2.6 \pm 0.3$ , and  $591.3 \pm 100.7$  nmol phosphate per min per mg kinase were incorporated into the N-terminal peptide by cdc2, GSK3, MEK1, P70S6K, CaMKII, PKA, and PKC $\alpha$ , respectively (see Experimental Procedures and the Supplemental Data).

phosphorylation of DAT N-terminal serines, we performed the same experiment with two DAT mutants: one in which Ser2, Ser4, Ser7, Ser12, and Ser13 were mutated simultaneously to alanines (S/A) to prevent phosphorylation, and one in which the same serines were mutated to aspartates to mimic their phosphorylated state (S/D). In S/A-expressing cells, we observed  $\sim 90\%$  reduction in AMPH-induced DAT-mediated currents and DA efflux, in accordance with our previous observations (Khoshbouei et al., 2004). In addition, AMPH-induced DA efflux by S/A was not stimulated by activated CaMKII $\alpha$  in the patch pipette (data not shown). In S/D-expressing cells, which display AMPH-induced DA efflux similar to wt (Khoshbouei et al., 2004), activated CaMKII $\alpha$  also failed to significantly affect DA efflux (Figure 5B, left panels) or the whole-cell currents (Figure 5B, right panels) at all voltages tested. This suggests that the stimulatory effect of CaMKII $\alpha$  occurs via phosphorylation of one or more the five N-terminal serines. This phosphorylation might be mediated directly by CaMKII $\alpha$ , although an indirect role of CaMKII $\alpha$  activation cannot be ruled out.

To assess the impact of N-terminal phosphorylation on DA efflux in the absence of AMPH, we compared basal efflux in cells expressing the DAT S/A mutant or the S/D mutant. Since these mutants display similar uptake properties (Khoshbouei et al., 2004) we could assume that dopamine preloading was similar in the two cell lines. Subsequent to loading (1  $\mu$ M DA for 45 min), the cells were washed, and basal efflux was measured by amperometry. The DAT-mediated basal DA efflux was defined as the efflux that could be inhibited by cocaine. As shown in Figure 4C, we observed substantially higher basal efflux in the S/D mutant as compared to the S/A mutant (Figure 5C); hence, N-terminal phosphorylation mimicked by the S to D substitutions was sufficient to drive efflux in the absence of AMPH in cells with physiological resting membrane potential and intracellular sodium concentration.

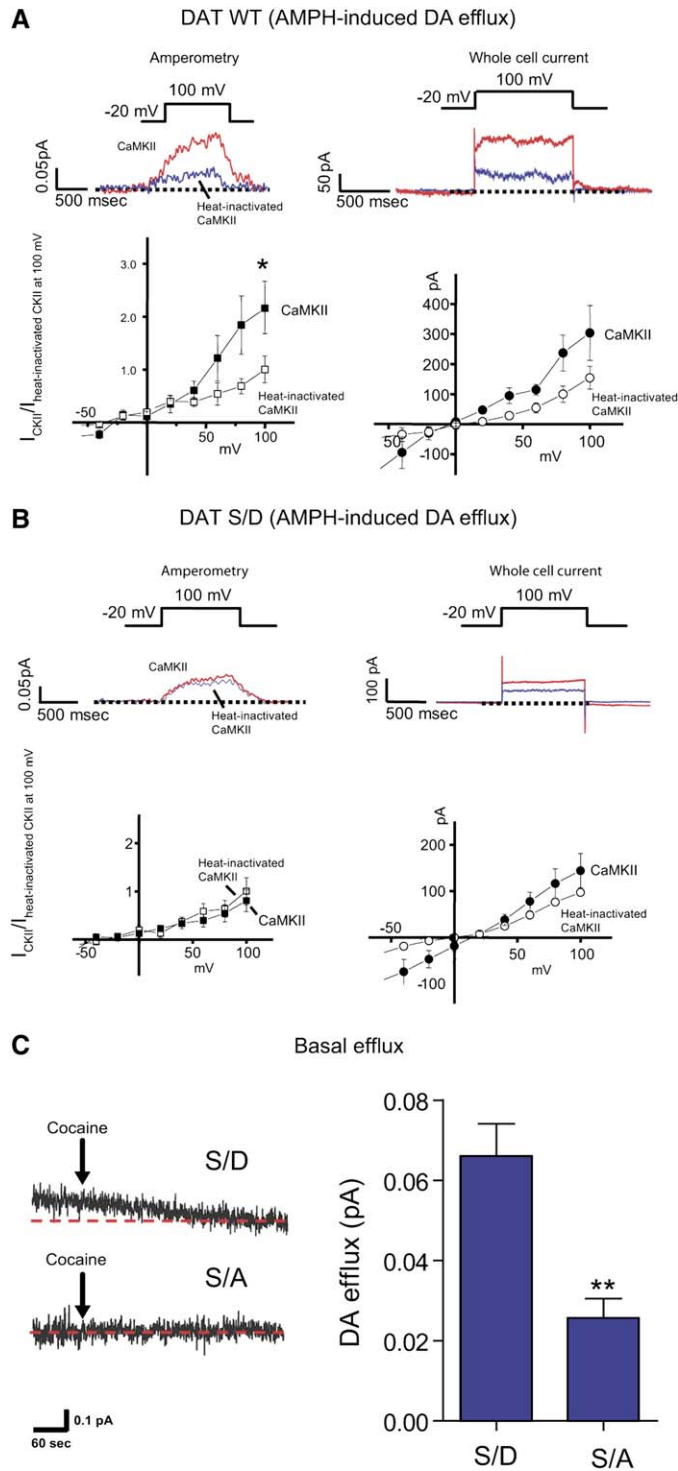


Figure 5. CaMKII $\alpha$  Stimulates AMPH-Induced Efflux of DA

(A) Application of monomeric activated CaMKII $\alpha$  via the whole-cell patch pipette increases AMPH-induced DA efflux and currents in EM4 cells expressing wild-type YFP DAT. Cells were voltage clamped with a patch pipette while an amperometric electrode was placed onto the cell membrane. The internal solution of the patch pipette contained 2 mM DA and 30 mM Na<sup>+</sup> (Kahlig et al., 2005). The AMPH-induced whole-cell and amperometric currents were defined as the current recorded in the presence of AMPH minus the current recorded after the addition of cocaine to the bath with AMPH still present. (Left panels) Representative trace (upper left) and corresponding amperometric-voltage relationships (lower left) of AMPH-induced oxidation current reflecting DA release obtained from YFP-DAT cells upon bath application of AMPH (10  $\mu$ M) and addition of either 0.45  $\mu$ M activated (red trace or closed symbols) or heat-inactivated (blue trace or open symbols) monomeric CaMKII $\alpha$  to the internal solution. To obtain the voltage relationships, the membrane potential was stepped from a holding potential of -20 mV to voltages between -40 mV and +100 mV in 20 mV increments (means  $\pm$  SE, n = 5–8). The amperometric-voltage relationships are normalized to the current observed at +100 mV with inactivated kinase ( $0.13 \pm 0.03$  pA) and are shown as means  $\pm$  SE, n = 5–8 (\*p < 0.05, one-way ANOVA followed by a post hoc Tukey Test). (Right panels) Representative current trace (upper right) and corresponding current-voltage relationships (lower right) of AMPH-induced whole-cell current acquired concomitantly to the oxidation current in the left panels (means  $\pm$  SE, n = 5–8).

(B) Application of monomeric activated CaMKII $\alpha$  does not increase AMPH-induced DA efflux and currents in EM4 cells expressing YFP DAT S/D (Ser2, Ser4, Ser7, Ser12, and Ser13 mutated to aspartates). (Left panels) Representative trace (upper left) and corresponding amperometric-voltage relationships (lower left) of AMPH-induced oxidation current reflecting DA release obtained from YFP-DAT S/D cells upon bath application of AMPH (10  $\mu$ M) and addition of either 0.45  $\mu$ M activated (red trace or closed symbols) or heat-inactivated (blue trace or open symbols) monomeric CaMKII $\alpha$  to the internal solution. The amperometric-voltage relationships are normalized to the current observed at 100 mV with inactivated kinase ( $0.14 \pm 0.04$  pA) and shown as means  $\pm$  SE, n = 4. (Right panels) Representative current trace (upper right) and corresponding current-voltage relationships (lower right) of AMPH-induced whole-cell current acquired concomitantly to the oxidation current in the left panels (means  $\pm$  SE, n = 4).

(C) Basal efflux from EM4 cells expressing YFP-DAT S/D (Ser2, Ser4, Ser7, Ser12, and Ser13 mutated to aspartates) or YFP-DAT S/A (Ser2, Ser4, Ser7, Ser12, and Ser13 mutated to alanines). Cells were preincubated with 1  $\mu$ M DA for 45 min. AMPH-independent DA efflux was measured by amperometry. DA efflux mediated by DAT was calculated by subtracting the efflux obtained in the presence of 10  $\mu$ M cocaine from the efflux under control conditions. (Left panels) Representative traces. (Right panels) DAT-mediated efflux in YFP-DAT S/D or YFP-DAT S/A calculated as described above. Data are represented as the mean  $\pm$  SE and were compared against each other using an unpaired Student's t test. (n = 7–10; \*\*p < 0.01).

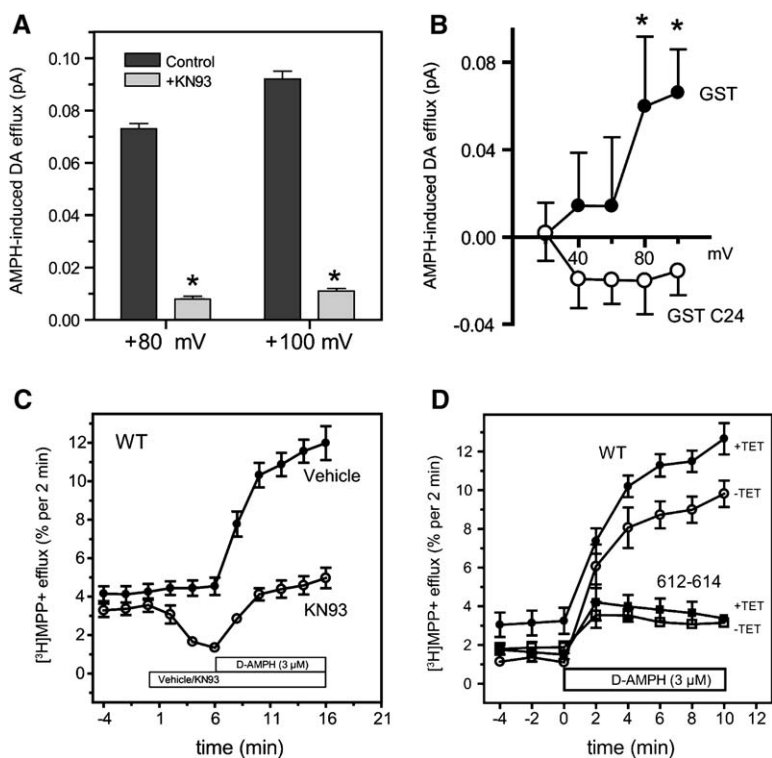


Figure 6. Role of the DAT C Terminus in AMPH-Induced DA Efflux  
(A) Effect of the CaMKII inhibitor KN93 on AMPH-induced efflux in EM4 cells stably expressing YFP-DAT using the experimental paradigm described in Figure 5. Data represent the DA efflux induced by 10  $\mu$ M AMPH at +80 and at +100 mV in the presence or absence of the CaMKII inhibitor KN93 (5  $\mu$ M) (means  $\pm$  SE,  $n = 5$ ,  $*p < 0.05$ ). No effect was observed with the inactive analog KN92 (data not shown).  
(B) The C-terminal DAT GST fusion protein C24 but not GST alone blocked AMPH-induced efflux in the YFP-DAT cells. Data represent the amperometric currents induced by 10  $\mu$ M AMPH at the indicated voltages with addition of 3  $\mu$ M GST DAT C24 or GST to the pipette (means  $\pm$  SE,  $n = 5$ ,  $*p < 0.05$ ). To obtain the voltage relationships, the membrane potential was stepped from a holding potential of  $-20$  mV to voltages between +20 mV and +100 mV in 20 mV increments.  
(C) Effect of the CaMKII inhibitor KN93 on AMPH-induced efflux in T-Rex HEK293 CaMKII $\alpha$ -FLAG hDAT cells induced with tetracycline (TET). Cells were preloaded with [ $^3$ H]MPP $^+$ , superfused, and the experiment was initiated with collection of 2 min fractions. AMPH was added after three fractions (6 min). (Vehicle) AMPH (3  $\mu$ M) was added at  $t = 6$  min. (KN93) KN93 (15  $\mu$ M) was added at  $t = 0$  min followed by AMPH (3  $\mu$ M) at  $t = 6$  min. Data are fractional release per 2 min in percent (means  $\pm$  SE of 12 observations from four experimental days). (D) AMPH-induced efflux without ( $-$ TET) and with ( $+$ TET) induction of CaMKII $\alpha$  expression with tetracycline in T-Rex HEK293 CaMKII $\alpha$  cells expressing FLAG hDAT or a mutant in which residues 612–614 were substituted with alanines (FLAG-hDAT 612–614). AMPH (3  $\mu$ M) was added at  $t = 0$  min. Data are fractional release per 2 min in percent (means  $\pm$  SE, 12 observations from four experimental days).

### AMPH-Induced DAT-Mediated DA Efflux Is Facilitated by Association of CaMKII $\alpha$ with the DAT C Terminus

For intracellular perfusion with the whole-cell patch pipette we were limited to the use of the monomeric form of CaMKII, which lacks the association domain, since full-length CaMKII $\alpha$  forms a dodecameric structure that is too large for diffusion from the pipette. Thus, the method did not allow us to address the importance of the binding between the association domain and the DAT C terminus. To study the significance of the interaction, we studied AMPH-induced DA efflux in DAT-expressing EM4 cells without any addition of activated CaMKII $\alpha$ . This efflux appeared to be dependent on endogenously expressed CaMKII $\alpha$  since it was almost eliminated by the specific CaMKII $\alpha$  inhibitor KN93 (Figure 6A). We also observed that addition to the patch pipette of the C-terminal C24 DAT GST fusion protein (3  $\mu$ M), which would compete with the C terminus of DAT for binding to CaMKII $\alpha$ , acted as a dominant-negative regulator and eliminated AMPH-induced DA efflux (Figure 6B). In contrast, a corresponding concentration of GST alone maintained the AMPH-induced DA efflux (Figure 6B).

To corroborate these electrophysiological data in a different experimental paradigm, we studied the role of CaMKII $\alpha$  in regulating AMPH-induced radiolabeled substrate efflux in T-Rex HEK293 CaMKII $\alpha$  cells stably expressing DAT. In these cells, tetracycline markedly up-regulated CaMKII $\alpha$  expression as assessed by immunoblotting, without affecting DAT function as assessed by

uptake experiments (data not shown). We used a superfusion system that allows for continuous monitoring of efflux after preloading cells with radioactively labeled substrate (Pifl and Singer, 1999; Scholze et al., 2002; Sitte et al., 1998). We used [ $^3$ H]MPP $^+$ , a hydrophilic DAT substrate that is resistant to enzymatic degradation and exhibits minimal nonspecific diffusion out of the cell (Pifl and Singer, 1999; Scholze et al., 2002; Sitte et al., 1998). In tetracycline-induced cells, AMPH caused a dose-dependent increase in [ $^3$ H]MPP $^+$  efflux, which reached a maximum in the presence of 3  $\mu$ M AMPH (Figure 6C and data not shown). Importantly, both the basal and the AMPH-induced efflux of [ $^3$ H]MPP $^+$  were markedly decreased by the specific CaMKII $\alpha$  inhibitor KN93 (Figure 6C).

We also stably expressed in the T-Rex HEK293 CaMKII $\alpha$  cells a DAT mutant in which residues 612–614 were substituted with alanines. Based on our pull-down data, this mutation should reduce the affinity of the DAT C terminus for CaMKII $\alpha$  (Figure 1). Note that the other DAT mutant that displayed reduced CaMKII $\alpha$  binding (DAT 615–617) (Figure 1) could not be used because of decreased expression (Bjerggaard et al., 2004). Basal efflux in both the wild-type and 612–614 mutant cell lines was identical when CaMKII $\alpha$  expression was not induced with tetracycline (Figure 6D). However, whereas tetracycline induction increased basal efflux in the wild-type, we observed no effect in the 612–614 mutant (Figure 6D). Furthermore, in contrast to wild-type DAT, induction of CaMKII $\alpha$  expression had no effect on AMPH-induced efflux in the 612–614 mutant (Figure 6D).

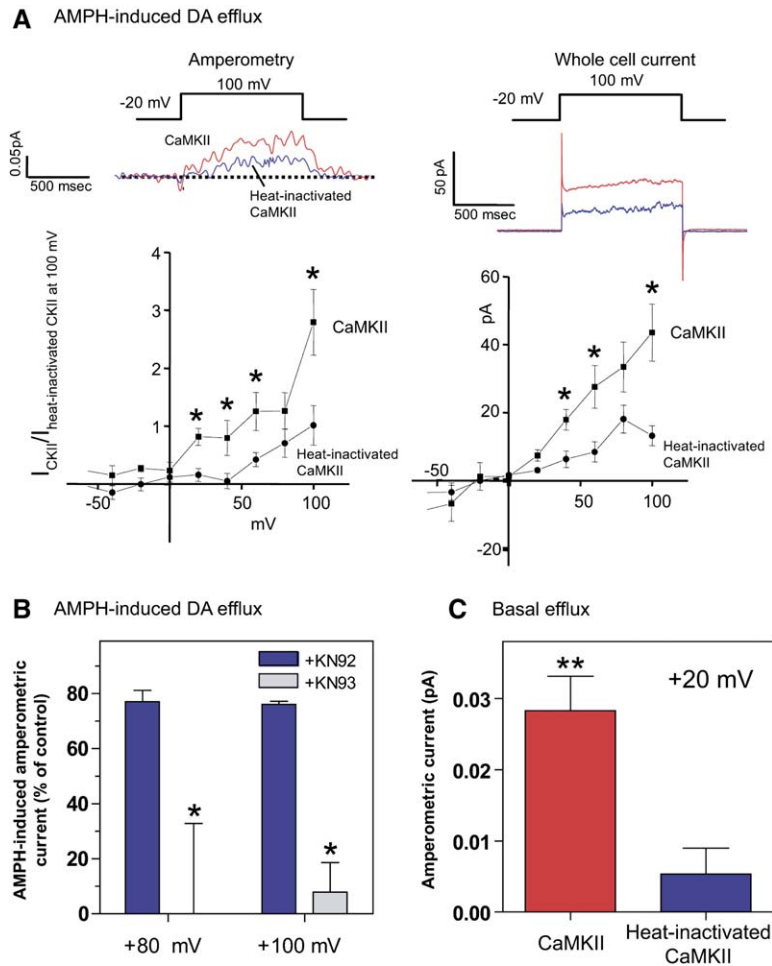


**Figure 7. CaMKII $\alpha$  Stimulates AMPH-Induced Efflux in Midbrain Dopaminergic Neurons**

(A) Application of monomeric activated CaMKII $\alpha$  via the whole-cell patch pipette increases AMPH-induced DA efflux and currents in mouse midbrain dopaminergic neurons, using the experimental paradigm described in Figure 5. (Left panels) Representative trace (upper left) and corresponding amperometric-voltage relationships (lower left) of AMPH-induced oxidation current reflecting DA release obtained from neurons upon bath application of AMPH (10  $\mu$ M) and addition of either 0.225  $\mu$ M activated (red trace or closed squares) or heat-inactivated (blue trace or closed circles) CaMKII $\alpha$  to the internal solution. To obtain the voltage relationships the membrane potential was stepped from a holding potential of  $-20$  mV to voltages between  $-40$  mV and  $+100$  mV in 20 mV increments (means  $\pm$  SE,  $n = 5-8$ ). The amperometric-voltage relationships are normalized to the current observed at  $+100$  mV with inactivated kinase ( $0.04 \pm 0.015$  pA) and shown as means  $\pm$  SE,  $n = 3-4$  (\* $p < 0.05$ , one-way ANOVA followed by a post hoc Tukey test). (Right panels) Representative current trace (upper right) and corresponding current-voltage relationships (lower right) of AMPH-induced whole-cell current acquired concomitantly to the oxidation current in the left panels (means  $\pm$  SE,  $n = 3-4$ ).

(B) Effect of the CaMKII inhibitor KN93 on AMPH-induced efflux in mouse midbrain dopaminergic neurons. AMPH-induced amperometric currents (means  $\pm$  SE,  $n = 3-4$ , \* $p < 0.05$ ) recorded at  $+80$  and at  $+100$  mV in the presence of KN92 (5  $\mu$ M) or KN93 (5  $\mu$ M) were normalized to vehicle controls at each potential.

(C) Basal DA efflux in dopaminergic neurons, determined by subtracting the amperometric current obtained in the presence of 10  $\mu$ M cocaine from that obtained with either 0.225  $\mu$ M activated or heat-inactivated CaMKII $\alpha$  in the patch pipette at a membrane potential of  $+20$  mV. Data are means  $\pm$  SE of  $n = 7-8$  (\*\* $p < 0.01$ , unpaired Student's  $t$  test).

The magnitude of the AMPH-induced efflux was also much lower (10%–20% of wt) in the mutant, regardless of the state of induction (Figure 6D). This reduced efflux is unlikely to be due to altered functional expression of the mutant as [ $^3$ H]DA uptake was  $71\% \pm 2\%$  (mean  $\pm$  SE,  $n = 5$ ) of that of the wild-type in the stably transfected pool clones.

#### Inhibition of CaMKII $\alpha$ Reduces AMPH-Induced DAT-Mediated DA Efflux in Midbrain DA Cultured Neurons, Striatal Brain Slices, and in the Striatum of Living Mice

We assessed the importance of CaMKII $\alpha$  for AMPH-induced DA efflux in a more physiological context by investigating AMPH-induced DAT-mediated DA efflux in mouse midbrain DA neurons in culture using the amperometry/whole-cell patch-clamp technique described above. Similar to our findings in heterologous cells, activated CaMKII $\alpha$  augmented significantly AMPH-induced DA efflux (Figure 7A, left panels) as well as the parallel whole-cell currents (Figure 7A, right panels) as compared to heat-inactivated CaMKII $\alpha$ . Representative traces are shown in the upper panels, whereas the corresponding current-voltage relationships for the

amperometric and whole currents are shown in the lower panels of Figure 7A. With the same experimental configuration, but without activated kinase in the pipette, the specific CaMKII inhibitor KN93 (5  $\mu$ M) essentially abolished AMPH-induced DA efflux (Figure 7B). In contrast, the inactive analog KN92 had no significant effect (Figure 7B).

To investigate whether CaMKII $\alpha$  can promote DA efflux also in the absence of AMPH, and thus under more physiological conditions, we assessed the effect of CaMKII $\alpha$  at a membrane potential of  $+20$  mV, a potential reached during physiological neuronal stimulation. These data showed that active, but not heat-inactivated, CaMKII $\alpha$  can stimulate efflux of DA independently from AMPH (Figure 7C), at least under these experimental conditions.

Further support for a critical role of CaMKII in the native setting was obtained by studying DA efflux in rat striatal slices using the superfusion system described above (Pifl and Singer, 1999; Scholze et al., 2002; Sitte et al., 1998). As shown in Figure 8A, AMPH caused a profound efflux of [ $^3$ H]MPP $^+$  from the preloaded slices, and KN93 markedly inhibited this efflux. A trend toward inhibition of basal efflux by KN93 was also observed.



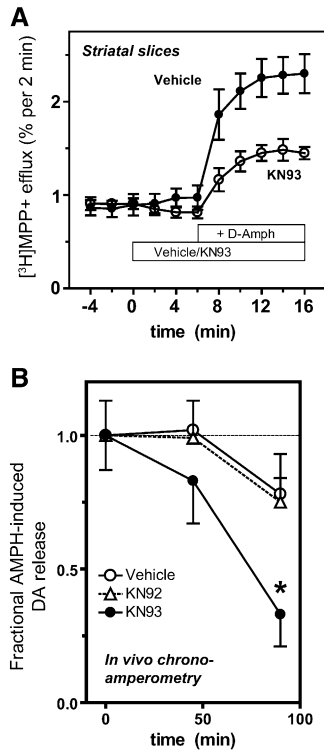


Figure 8. The CaMKII Inhibitor KN93 Decreases Efflux in Striatal Brain Slices and in the Striatum of Living Mice

(A) The effect of the CaMKII $\alpha$  inhibitor KN93 on AMPH-induced efflux of the DAT substrate [ $^3$ H]MPP $^+$  in striatal slices. The slices were pre-loaded with [ $^3$ H]MPP $^+$ , superfused, and 2 min fractions were collected. (Vehicle) AMPH (3  $\mu$ M) was added at t = 6 min; (KN93) KN93 (15  $\mu$ M) was added at t = 0 min followed by AMPH (3  $\mu$ M) at t = 6 min. Data are fractional release per 2 min in percent (means  $\pm$  SE, 12 observations, one observation equals one superfusion chamber).

(B) The effect of KN93 on DA efflux induced by locally applied AMPH in the striatum of anesthetized mice as assessed by *in vivo* high-speed chronoamperometry. Data are presented as fractional AMPH-induced DA efflux after locally applied vehicle (aCSF) (open circles), KN92 (open triangles), or KN93 (closed circles) relative to the pretreatment AMPH-induced DA efflux (means  $\pm$  SE, \* $p$  < 0.05 versus vehicle). Pretreatment values were  $0.81 \pm 0.13$  micromolar DA (n = 14),  $0.92 \pm 0.22$  micromolar DA (n = 6), and  $0.89 \pm 0.23$  micromolar DA (n = 9) for vehicle (aCSF), KN92, and KN93 treated mice, respectively.

Finally, we used high-speed chronoamperometry in mouse striatum (Callaghan et al., 2005; Montanez et al., 2003) to assess *in vivo* the effect of the CaMKII inhibitor KN93 on AMPH-induced efflux of endogenous DA. AMPH-induced DA efflux was not significantly altered 45 and 90 min after local microinjection of vehicle (artificial cerebral spinal fluid [aCSF]) or of KN92, the inactive analog of KN93 (Figure 8B). In contrast, local microinjection of KN93 significantly attenuated AMPH-induced DA efflux (ANOVA:  $F_{2,26} = 4.31$ ,  $p = 0.023$ ). Relative to aCSF, KN93 decreased AMPH-induced DA release by 27% at 45 min ( $p = 0.33$ , n = 9–14) and by 67% at 90 min ( $p < 0.05$ , n = 9–14) (Figure 8B). Prior to KN93, KN92, or aCSF, AMPH induced DA release in all mice. AMPH continued to evoke DA efflux at 90 min in 13 of 14 (93%) and 6 of 6 (100%) mice treated with aCSF and KN-92, respectively. However, 90 min follow-

ing KN93, AMPH-evoked DA efflux was only detected in 4 of 9 mice (56%).

## Discussion

Like other Na $^+$ -coupled transporters, DAT is capable not only of mediating Na $^+$ -coupled uptake but also of transporting substrate in the reverse direction. The reverse transport, or efflux, of DA through DAT seen in response to AMPHs is believed to play a significant role in the addictive and reinforcing properties of these compounds (Sulzer et al., 2005). Recently, we discovered that phosphorylation of N-terminal serines mediates the reversal of transport in response to AMPHs (Khoshbouei et al., 2004). Thus, N-terminal phosphorylation shifts DAT from a “reluctant” to a “willing” state for AMPH-induced efflux (Khoshbouei et al., 2004). Consistent with this hypothesis, AMPH and methamphetamine increase phosphorylation of DAT both *in vivo* and *in vitro* (Cervinski et al., 2005), and truncation of the distal 21 N-terminal residues in DAT prevent this phosphorylation (Cervinski et al., 2005), in agreement with AMPH-induced phosphorylation of N-terminal serines.

In the present paper we identify CaMKII as key player in AMPH-induced DA efflux. We provide data supporting an interaction of the CaMKII $\alpha$  association domain with the C terminus of DAT, which might operate to increase the likelihood that the kinase domain will phosphorylate serines in the N terminus and thus promote AMPH-induced DA efflux. First, in a yeast two-hybrid screen we identified CaMKII $\alpha$  as a putative interaction partner for the DAT C terminus. Second, we confirmed and mapped the interaction to discrete residues in the distal C terminus using pull-down and coimmunoprecipitation experiments. Third, we confirmed that CaMKII $\alpha$  and DAT are coexpressed and colocalize in dopaminergic neurons in primary culture. Fourth, we demonstrated that CaMKII can phosphorylate *in vitro* a synthetic DAT N-terminal peptide. Fifth, by using an array of different techniques in heterologous cells, dopaminergic neurons, striatal brain slices, and living animals, we demonstrated a key role for CaMKII $\alpha$  in AMPH-induced DA efflux. Finally, we obtained evidence that binding of the kinase to the DAT C terminus is an important element in the pathway by using a C-terminal DAT GST fusion protein (C24) to decrease CaMKII $\alpha$  binding to DAT or by using a mutant DAT with impaired ability to bind CaMKII $\alpha$ . Although in the whole-cell patch-clamp/ampereometry setup, addition of activated monomeric CaMKII $\alpha$  lacking the association domain still stimulated efflux, this likely results because the concentration of the activated kinase at the plasma membrane, when added with the patch pipette, is sufficient to substitute for the lack of its interaction with the C terminus of DAT.

It is conceivable that our proposed role for CaMKII $\alpha$  to mediate DA efflux in response to AMPH also is important under physiological conditions. Indeed, DAT has been proposed to play a role in nonvesicular release of DA in the substantia nigra upon excitation of glutamatergic neurons projecting from the subthalamic nucleus through a mechanism involving membrane depolarization and changes in the ionic gradient (Falkenburger et al., 2001). Consistent with this possibility, we demonstrated that activated CaMKII $\alpha$ , which would result from

neuronal depolarization and increased  $\text{Ca}^{2+}$  (Colbran, 2003; Griffith, 2004), can stimulate DA efflux in dopaminergic neurons in the absence of AMPH at +20 mV, a potential reached during physiological neuronal stimulation (Figure 7C). We should note that in the absence of AMPH, 2 mM is a high intracellular DA concentration; however, we have shown previously that the properties of DA efflux at this concentration are similar to those obtained at much lower intracellular DA concentrations (Kahlig et al., 2005). To obtain a sufficient signal-to-noise ratio in DA neurons, which have very small amperometric currents, we therefore used this high intracellular DA concentration. The experiments were also performed in the presence of a relatively high concentration of intracellular sodium (30 mM). However, intracellular sodium can rise appreciably during neuronal activity: for example, a tetanic stimulus that is typically used to trigger long-term potentiation has been shown to increase the intracellular sodium concentration to as much as 45 mM within the shafts of dendrites and to over 100 mM in active dendritic spines (Rose and Konnerth, 2001). Moreover, recovery to baseline sodium levels, which is mediated by the plasma membrane  $\text{Na}^+/\text{K}^+$ -ATPase, is very slow, typically requiring tens of seconds (Rose, 2002).

Our data obtained in cells preloaded with [ $^3\text{H}$ ]MPP provided further support for the notion that efflux through DAT can occur in a  $\text{CaMKII}\alpha$ -dependent manner without AMPH, since KN93 potently inhibited basal efflux of [ $^3\text{H}$ ]MPP preloaded cells expressing the hDAT (Figure 6C). In addition, induction of  $\text{CaMKII}$  expression enhanced basal efflux of [ $^3\text{H}$ ]MPP $^+$  in the wild-type but not in cells expressing a transporter with impaired  $\text{CaMKII}$  binding (Figure 6D). We also show that pseudophosphorylation of the hDAT N-terminal serines (S/D mutation), which appear to be phosphorylated by  $\text{CaMKII}\alpha$ , causes reverse transport of DA at resting membrane potential in unclamped cells, thereby mimicking what could happen upon  $\text{CaMKII}$  activation in the absence of amphetamine (Figure 5C).

An interesting question is how N-terminal phosphorylation mechanistically is coupled to stimulation of DA efflux. We have shown previously that pseudophosphorylation of the DAT N terminus (S/D mutant) does not affect the rate of substrate accumulation of substrate in unclamped cells (Khoshbouei et al., 2004). Therefore, at least in unclamped cells, N-terminal phosphorylation alters the rate of efflux without altering the reuptake of DA. Nevertheless, despite that the rate of uptake appears to be unaltered in the mutant, it is possible that phosphorylation might alter the ionic coupling of DAT. The ratio of whole-cell to amperometric current was, however, not altered by preventing phosphorylation (Khoshbouei et al., 2004). This ratio is a microscopic property of an individual transporter that is inversely proportional to the fraction of charge carried by substrate (Galli et al., 1997). The data are consistent, therefore, with a similar ionic coupling in the presence or absence of N-terminal phosphorylation.

Earlier studies indicated a role of  $\text{CaMKII}$  in AMPH-induced efflux, but only after psychostimulant sensitization (Kantor et al., 1999; Pierce and Kalivas, 1997), whereas we have demonstrated a role for  $\text{CaMKII}$  in the acute response to AMPH. Most likely this results from

differences in the experimental approaches: Kantor et al. used substantially larger striatal slices and a slower perfusion (Kantor et al., 1999), and for the in vivo experiments we used high-speed chronoamperometry, which has a high time resolution, instead of microdialysis (Kantor et al., 1999; Pierce and Kalivas, 1997). Previous studies have also suggested involvement of PKC in AMPH-induced efflux. Measurements in striatal slices and microdialysis experiments in nucleus accumbens showed that AMPH-induced DA efflux in naive and in behaviorally sensitized animals was decreased by PKC inhibitors (Kantor et al., 1999; Pierce and Kalivas, 1997). Additionally, the increase in phosphorylation of N-terminal serines in DAT seen in response to AMPHs is decreased by a high concentration of the PKC inhibitor GF109230X (Cervinski et al., 2005) and phosphorylation of the N-terminal serines is promoted by PKC activators such as PMA (Granás et al., 2003). Recent data have moreover suggested a particular role of the  $\text{PKC}\beta$  isoform (Johnson et al., 2005). The present data also do not exclude a role of PKC. In fact, we show that the DAT N terminus is a substrate for  $\text{PKC}\alpha$ , at least in vitro, and the PKC inhibitor GF109230X inhibited AMPH-induced efflux of [ $^3\text{H}$ ]MPP $^+$  from striatal slices to a similar extent as KN93 (data not shown). In contrast, the effect of the PKC inhibitor was markedly smaller than that of KN93 in cells cotransfected with DAT and  $\text{CaMKII}\alpha$  (data not shown), and we observed no effect of GF109230X (1  $\mu\text{M}$ ) on the increase in DA efflux observed when autoactivated  $\text{CaMKII}\alpha$  was added to the patch pipette (data not shown). Thus, although interplay between PKC and  $\text{CaMKII}\alpha$  is possible, our data suggest that  $\text{CaMKII}$  mediation of AMPH-induced DA efflux is independent of PKC.

$\text{CaMKII}$  is the most abundant kinase in the brain and plays major roles in regulation of complex cognitive and behavioral functions, including synaptic plasticity (Colbran, 2003; Griffith, 2004). Activation of the kinase occurs upon local increases in  $\text{Ca}^{2+}$  concentration and involves binding of the  $\text{Ca}^{2+}$ /calmodulin complex to the regulatory domain (Colbran, 2003; Griffith, 2004).  $\text{CaMKII}$  is well known to interact with several proteins important for neuronal signal transduction. Most proteins, including the NR2B subunit of the NMDA receptor and  $\alpha$ -actinin bind the catalytic or regulatory domain (Colbran, 2003; Griffith, 2004). In contrast, densin-180 interacts with the C-terminal association domain that also is known to be involved in oligomerization of the enzyme (Robison et al., 2005). Functionally, the interaction with densin-180 is believed to play a significant role in determining the subcellular localization of  $\text{CaMKII}\alpha$ , with little effect on catalytic activity (Robison et al., 2005). The present data identifies DAT as another interaction partner of the  $\text{CaMKII}\alpha$  association domain, linking the binding of  $\text{CaMKII}\alpha$  to DAT with the neurobiology of AMPH.

#### Experimental Procedures

##### Yeast Two-Hybrid Screen

The yeast two-hybrid screen was performed using the HybridHunter system (Invitrogen) as described in the Supplemental Data. The 46 C-terminal residues of the human DAT (hDAT) were used as bait against a human brain cDNA library.

### DNA Constructs and Mutagenesis

The GST fusion proteins containing positions 597–620 (C24), 575–620 (C46), 581–620 (C40), and 581–609 (C40del11) of the hDAT and positions 594–617 of NET and 607–630 of SERT were generated as described in the [Supplemental Data](#). For stable or transient expression of the hDAT, we used either synDAT (a synthetic human DAT gene) in pcDNA3 (Loland et al., 2004), synDAT with an N-terminal FLAG tag in the bicistronic vector pCIN4, or synDAT tagged at the N terminus with yellow fluorescent protein in the bicistronic vector pChygro (Saunders et al., 2000). The hDAT constructs in which Ser2, Ser4, Ser7, Ser12, and Ser13 were mutated to alanines (S/A) and aspartate (S/D) were generated as described (Khoshbouei et al., 2004). See the [Supplemental Data](#) for details.

### Cell Culture and Transfection

EM4 cells, HEK293 cells stably transfected with macrophage scavenger receptor to promote adherence, were grown as described (Khoshbouei et al., 2004). T-Rex HEK293 cells (human embryonic kidney) (Invitrogen) with stable expression of Tet repressor from pcDNA6/TR were grown as EM4 cells except that 5  $\mu$ g/ml blasticidin and 175  $\mu$ g/ml hygromycin were added to the media. Transfections were performed with the Lipofectamine 2000 transfection kit (Invitrogen).

### Neuronal Cultures

Postnatally derived rat midbrain dopaminergic neurons were isolated and grown as described in the [Supplemental Data](#), modified from Rayport et al. (1992). Mouse midbrain dopaminergic neurons were prepared as described in the [Supplemental Data](#).

### In Vitro Binding Assays

Purified murine CaMKII $\alpha$  was autophosphorylated in the presence of 2  $\mu$ M calmodulin and [ $^{32}$ P]- $\gamma$ -ATP (Amersham Biosciences) and incubated with hDAT, hNET, or hSERT GST fusion proteins on glutathione beads for 30 min at 37°C. The beads were washed with ice-cold TBS with 0.1% Triton X-100 before elution and detection of binding by SDS-PAGE and autoradiography. For detection of binding to CaMKII $\alpha$  expressed in cells, lysates from CaMKII $\alpha$  T-Rex HEK293 cells induced with tetracycline were incubated with DAT GST fusion proteins as indicated. The beads were washed before elution and analysis by SDS-PAGE/immunoblotting. For detection of binding to endogenously expressed CaMKII $\alpha$ , crude PSDs from rat brains were prepared (Gardoni et al., 1999). PSDs were solubilized in TBS with 0.1% SDS, diluted in TBS, and incubated with hDAT GST fusion proteins. The beads were washed before elution and analysis by SDS-PAGE/immunoblotting. See the [Supplemental Data](#) for details.

### Immunoprecipitations

Lysates from T-Rex HEK293 CaMKII $\alpha$  cells, stably or transiently expressing hDAT or *c-myc*-tagged hSERT (prepared in TBS containing 1% [v/v] Triton X-100, 5 mM N-ethylmaleimide, 200  $\mu$ M PMSF, and a protease inhibitor cocktail [Roche Diagnostics]) were incubated with either 1  $\mu$ l rat MAB369 DAT antibody or 1  $\mu$ l goat CaMKII $\alpha$  antibody for 1 hr at 4°C. Formed complexes were isolated with Protein G agarose followed by SDS-PAGE and immunoblotting. See the [Supplemental Data](#) for details.

### Immunocytochemistry and Confocal Microscopy

Immunostaining was performed as described (Bjerggaard et al., 2004). Dopaminergic neurons were fixed in 4% formaldehyde and blocked/permeabilized with blocking-permeabilizing solution (5% goat serum, 1% BSA, and 0.1% saponin in PBS buffer) followed by incubation with indicated primary antibodies (MAB369 rat anti-DAT antibody [Chemicon, Temecula, CA] 1:1000; rabbit anti-CaMKII [Santa Cruz] 1:300; rabbit anti VMAT2 [Pel-Freez Biologicals] 1:2000; rabbit anti-tyrosine hydroxylase [Affinity Bioreagents] 1:1000). Secondary antibodies used included goat anti-rat Alexa Fluor 488 (1:1000) and goat anti-rabbit Alexa Fluor 568 (Molecular Probes). Stained cells were visualized using a Zeiss LSM 510 confocal laser scanning microscope with an oil-immersion 63 $\times$  objective.

### In Vitro Phosphorylation

Indicated protein kinases (50 ng) were incubated with 50  $\mu$ M of a peptide corresponding to the first 27 residues of hDAT (NH<sub>2</sub>-MSK SKC SVG LMS SVV APA KEP NAV GPK RR amide) or the indicated concentrations of the appropriate positive control substrates in the presence of 10 mM Mg<sup>2+</sup> and 0.1 mM [ $\gamma$ - $^{32}$ P]ATP for 10 min at 30°C. Recombinant CaMKII $\alpha$  (Calbiochem) was incubated in the presence of 0.4 mM CaCl<sub>2</sub> and 0.1 mg/ml calmodulin. After the incubation the mixture was filtered, washed, and counted for incorporated  $^{32}$ P. Note that the peptide contained two additional Arg residues at the C terminus to facilitate its binding to the negatively charged filter. All kinases (except CaMKII $\alpha$ ) were obtained from the Department of Signal Transduction Therapy, University of Dundee. Phosphorylation of the N-terminal peptide was compared with that of the appropriate control substrates for each kinase, which included 30  $\mu$ M phospho glycogen synthase (GSK3), 30  $\mu$ M kemptide (LRRASLG) (PKA), 30  $\mu$ M crosstide (GRPTSSFAEG) (p70S6K), 50  $\mu$ M autocalmitide 2 (KKALRRQETVDAL-amide) (CaMKII), 0.2 mg/ml histone H1 (PKC and cdc2), and a coupled MAPK kinase assay (MEK1).

### Amperometry/Electrophysiology

Whole-cell and amperometric currents were recorded as described previously (Khoshbouei et al., 2004) in EM4 cells expressing YFP-hDAT, YFP-hDAT S/A, and YFP-hDAT S/D or in midbrain dopaminergic neuron. When noted, purified monomeric CaMKII $\alpha$  (residues 1–380), which was thiophosphorylated at Thr286 to be constitutively active and resistant to phosphatases, was added to the internal solution. In control experiments, an equal amount of heat-inactivated (treated at 70°C for 20 min) monomeric CaMKII $\alpha$  was added. See the [Supplemental Data](#) for details.

### Efflux Experiments

Efflux experiments were performed in a superfusion system as described using [ $^3$ H]MPP<sup>+</sup> as radioactive substrate (Piff and Singer, 1999; Scholze et al., 2002; Sitte et al., 1998). Efflux in striatal slices was performed essentially as described by Scholze et al. (Scholze et al., 2002) except that the experiments were performed without EDTA in the superfusion buffer. See the [Supplemental Data](#) for details.

### In Vivo High-Speed Chronoamperometry

In vivo high-speed chronoamperometry was performed as described (Callaghan et al., 2005; Daws et al., 2000; Montanez et al., 2003) on male C57BL/6J mice at 8–10 weeks of age. The electrochemical recording assembly consisted of a Nafion-coated, single carbon fiber electrode attached to a double-barrel micropipette filled with either AMPH (800  $\mu$ M, Sigma), KN93 (400  $\mu$ M Calbiochem), or aCSF vehicle (pH 7.4). KN93 did not itself produce an electrochemical signal in vitro. The electrode-micropipette recording assembly was lowered into the dorsal striatum of anesthetized mice before high-speed chronoamperometric recordings were made. AMPH (125 nM, 100 pmol) was applied into the striatum by pressure-ejection (5–25 psi for 0.25–3.0 s) to evoke release of endogenous DA. As soon as the DA was cleared from extracellular fluid (ECF), typically 5–30 min after AMPH-application, KN93 (125 nM, 50 pmol) or aCSF (125 nM) was locally applied to striatum (5–25 psi for 0.25–3.0 s), and 45 min and 90 min later the same amount of AMPH was again pressure-ejected. The placement of the electrode tip was verified histologically. AMPH-evoked DA efflux was analyzed using one-way analysis of variance (ANOVA) followed by Tukey's post hoc tests.

### Supplemental Data

The Supplemental Data for this article can be found online at <http://www.neuron.org/cgi/content/full/51/4/417/DC1>.

### Acknowledgments

We thank Lisbeth Andersen and Martha Bass for technical assistance and Dr. Jan Egebjerg and Kenneth L. Madsen for helpful comments. We thank Dr. David Sulzer for helpful comments and help setting up postnatal cultures of midbrain neurons. J.U.F. was the recipient of a fellowship supported by the Medicin Valley Academy and H. Lundbeck A/S. The work was supported in part by the National Institute of Health Grants P01 DA 12408 (U.G., A.G., and

J.A.J.), DA 11495 (J.A.J.), MH 57324 (J.A.J.), DA 13975 (A.G.), DA 14684 (A.G.), DA 18992 (L.C.D.), MH 63232 (R.J.C.), and EY 15815 (D.G.M.), the Danish Research Councils, the Lundbeck Foundation (U.G.), the Novo Nordic Foundation (U.G.), the A.P. Moeller Foundation (U.G.), and grant P17076-B02 by the Austrian Science Foundation/FWF (H.H.S.).

Received: January 10, 2006

Revised: May 24, 2006

Accepted: June 27, 2006

Published: August 16, 2006

## References

- Amara, S.G., and Kuhar, M.J. (1993). Neurotransmitter transporters: recent progress. *Annu. Rev. Neurosci.* **16**, 73–93.
- Bjerggaard, C., Fog, J., Hastrup, H., Madsen, K., Javitch, J.A., and Gether, U. (2004). Surface targeting of the dopamine transporter involves discrete epitopes in the distal carboxyterminus but occurs independently of canonical PDZ domain interactions. *J. Neurosci.* **24**, 7024–7036.
- Callaghan, P.D., Irvine, R.J., and Daws, L.C. (2005). Differences in the in vivo dynamics of neurotransmitter release and serotonin uptake after acute para-methoxyamphetamine and 3,4-methylenedioxymethamphetamine revealed by chronoamperometry. *Neurochem. Int.* **47**, 350–361.
- Cervinski, M.A., Foster, J.D., and Vaughan, R.A. (2005). Psychoactive substrates stimulate dopamine transporter phosphorylation and down regulation by cocaine sensitive and protein kinase C dependent mechanisms. *J. Biol. Chem.* **280**, 40442–40449.
- Chen, N.H., Reith, M.E., and Quick, M.W. (2004). Synaptic uptake and beyond: the sodium- and chloride-dependent neurotransmitter transporter family SLC6. *Pflugers Arch.* **447**, 519–531.
- Colbran, R.J. (2003). Targeting of calcium/calmodulin-dependent protein kinase II. *Biochem. J.* **378**, 1–16.
- Daws, L.C., Irvine, R.J., Callaghan, P.D., Toop, N.P., White, J.M., and Bochner, F. (2000). Differential behavioural and neurochemical effects of para-methoxyamphetamine and 3,4-methylenedioxymethamphetamine in the rat. *Prog. Neuropsychopharmacol. Biol. Psychiatry* **24**, 955–977.
- Falkenburger, B.H., Barstow, K.L., and Mintz, I.M. (2001). Dendro-dendritic inhibition through reversal of dopamine transport. *Science* **293**, 2465–2470.
- Fischer, J.F., and Cho, A.K. (1979). Chemical release of dopamine from striatal homogenates: evidence for an exchange diffusion model. *J. Pharmacol. Exp. Ther.* **208**, 203–209.
- Galli, A., Petersen, C.I., deBlaquiere, M., Blakely, R.D., and DeFelice, L.J. (1997). Drosophila serotonin transporters have voltage-dependent uptake coupled to a serotonin-gated ion channel. *J. Neurosci.* **17**, 3401–3411.
- Gardoni, F., Schrama, L.H., van Dalen, J.J., Gispen, W.H., Cattabeni, F., and Di Luca, M. (1999). AlphaCaMKII binding to the C-terminal tail of NMDA receptor subunit NR2A and its modulation by autophosphorylation. *FEBS Lett.* **456**, 394–398.
- Gnegy, M.E. (2003). The effect of phosphorylation on amphetamine-mediated outward transport. *Eur. J. Pharmacol.* **479**, 83–91.
- Gnegy, M.E., Khoshbouei, H., Berg, K.A., Javitch, J.A., Clarke, W.P., Zhang, M., and Galli, A. (2004). Intracellular Ca<sup>2+</sup> regulates amphetamine-induced dopamine efflux and currents mediated by the human dopamine transporter. *Mol. Pharmacol.* **66**, 137–143.
- Granás, C., Ferrer, J., Loland, C.J., Javitch, J.A., and Gether, U. (2003). N-terminal truncation of the dopamine transporter abolishes phorbol ester- and substance P receptor-stimulated phosphorylation without impairing transporter internalization. *J. Biol. Chem.* **278**, 4990–5000.
- Griffith, L.C. (2004). Regulation of calcium/calmodulin-dependent protein kinase II activation by intramolecular and intermolecular interactions. *J. Neurosci.* **24**, 8394–8398.
- Iwata, S.I., Hewlett, G.H., Ferrell, S.T., Kantor, L., and Gnegy, M.E. (1997). Enhanced dopamine release and phosphorylation of synap-sin I and neuromodulin in striatal synaptosomes after repeated amphetamine. *J. Pharmacol. Exp. Ther.* **283**, 1445–1452.
- Jardetzky, O. (1966). Simple allosteric model for membrane pumps. *Nature* **211**, 969–970.
- Johnson, L.A., Guptaroy, B., Lund, D., Shamban, S., and Gnegy, M.E. (2005). Regulation of amphetamine-stimulated dopamine efflux by protein kinase C beta. *J. Biol. Chem.* **280**, 10914–10919.
- Kahlig, K.M., Binda, F., Khoshbouei, H., Blakely, R.D., McMahon, D.G., Javitch, J.A., and Galli, A. (2005). Amphetamine induces dopamine efflux through a dopamine transporter channel. *Proc. Natl. Acad. Sci. USA* **102**, 3495–3500.
- Kantor, L., Hewlett, G.H., and Gnegy, M.E. (1999). Enhanced amphetamine- and K<sup>+</sup>-mediated dopamine release in rat striatum after repeated amphetamine: differential requirements for Ca<sup>2+</sup>- and calmodulin-dependent phosphorylation and synaptic vesicles. *J. Neurosci.* **19**, 3801–3808.
- Khoshbouei, H., Wang, H., Lechleiter, J.D., Javitch, J.A., and Galli, A. (2003). Amphetamine-induced dopamine efflux. A voltage-sensitive and intracellular Na<sup>+</sup>-dependent mechanism. *J. Biol. Chem.* **278**, 12070–12077.
- Khoshbouei, H., Sen, N., Guptaroy, B., Johnson, L., Lund, D., Gnegy, M.E., Galli, A., and Javitch, J.A. (2004). N-terminal phosphorylation of the dopamine transporter is required for amphetamine-induced efflux. *PLoS Biol.* **2**, E78.
- Lieberman, J.A., Sheitman, B.B., and Kinon, B.J. (1997). Neurochemical sensitization in the pathophysiology of schizophrenia: deficits and dysfunction in neuronal regulation and plasticity. *Neuropsychopharmacology* **17**, 205–229.
- Loland, C.J., Norgaard-Nielsen, K., and Gether, U. (2003). Probing dopamine transporter structure and function by Zn<sup>2+</sup>-site engineering. *Eur. J. Pharmacol.* **479**, 187–197.
- Loland, C.J., Granás, C., Javitch, J.A., and Gether, U. (2004). Identification of intracellular residues in the dopamine transporter critical for regulation of transporter conformation and cocaine binding. *J. Biol. Chem.* **279**, 3228–3238.
- Montanez, S., Owens, W.A., Gould, G.G., Murphy, D.L., and Daws, L.C. (2003). Exaggerated effect of fluvoxamine in heterozygote serotonin transporter knockout mice. *J. Neurochem.* **86**, 210–219.
- Pierce, R.C., and Kalivas, P.W. (1997). Repeated cocaine modifies the mechanism by which amphetamine releases dopamine. *J. Neurosci.* **17**, 3254–3261.
- Piffl, C., and Singer, E.A. (1999). Ion dependence of carrier-mediated release in dopamine or norepinephrine transporter-transfected cells questions the hypothesis of facilitated exchange diffusion. *Mol. Pharmacol.* **56**, 1047–1054.
- Rawson, R.A., Gonzales, R., and Brethen, P. (2002). Treatment of methamphetamine use disorders: an update. *J. Subst. Abuse Treat.* **23**, 145–150.
- Rayport, S., Sulzer, D., Shi, W.X., Sawasdikosol, S., Monaco, J., Batson, D., and Rajendran, G. (1992). Identified postnatal mesolimbic dopamine neurons in culture: morphology and electrophysiology. *J. Neurosci.* **12**, 4264–4280.
- Robison, A.J., Bass, M.A., Jiao, Y., MacMillan, L.B., Carmody, L.C., Bartlett, R.K., and Colbran, R.J. (2005). Multivalent interactions of calcium/calmodulin-dependent protein kinase II with the postsynaptic density proteins NR2B, densin-180, and alpha-actinin-2. *J. Biol. Chem.* **280**, 35329–35336.
- Rose, C.R. (2002). Na<sup>+</sup> signals at central synapses. *Neuroscientist* **8**, 532–539.
- Rose, C.R., and Konnerth, A. (2001). NMDA receptor-mediated Na<sup>+</sup> signals in spines and dendrites. *J. Neurosci.* **21**, 4207–4214.
- Saunders, C., Ferrer, J.V., Shi, L., Chen, J., Merrill, G., Lamb, M.E., Leeb-Lundberg, L.M., Carvelli, L., Javitch, J.A., and Galli, A. (2000). Amphetamine-induced loss of human dopamine transporter activity: an internalization-dependent and cocaine-sensitive mechanism. *Proc. Natl. Acad. Sci. USA* **97**, 6850–6855.
- Scholze, P., Norregaard, L., Singer, E.A., Freissmuth, M., Gether, U., and Sitte, H.H. (2002). The role of zinc ions in reverse transport mediated by monoamine transporters. *J. Biol. Chem.* **276**, 40476–40485.

- Sitte, H.H., Huck, S., Reither, H., Boehm, S., Singer, E.A., and Piffl, C. (1998). Carrier-mediated release, transport rates, and charge transfer induced by amphetamine, tyramine, and dopamine in mammalian cells transfected with the human dopamine transporter. *J. Neurochem.* *71*, 1289–1297.
- Strack, S., Robison, A.J., Bass, M.A., and Colbran, R.J. (2000). Association of calcium/calmodulin-dependent kinase II with developmentally regulated splice variants of the postsynaptic density protein densin-180. *J. Biol. Chem.* *275*, 25061–25064.
- Sulzer, D., Sonders, M.S., Poulsen, N.W., and Galli, A. (2005). Mechanisms of neurotransmitter release by amphetamines: A review. *Prog. Neurobiol.* *75*, 406–433.
- Torres, G.E., Yao, W.D., Mohn, A.R., Quan, H., Kim, K.M., Levey, A.I., Staudinger, J., and Caron, M.G. (2001). Functional interaction between monoamine plasma membrane transporters and the synaptic PDZ domain-containing protein PICK1. *Neuron* *30*, 121–134.
- Torres, G.E., Gainetdinov, R.R., and Caron, M.G. (2003). Plasma membrane monoamine transporters: structure, regulation and function. *Nat. Rev. Neurosci.* *4*, 13–25.
- Walikonis, R.S., Oguni, A., Khorosheva, E.M., Jeng, C.J., Asuncion, F.J., and Kennedy, M.B. (2001). Densin-180 forms a ternary complex with the (alpha)-subunit of Ca<sup>2+</sup>/calmodulin-dependent protein kinase II and (alpha)-actinin. *J. Neurosci.* *21*, 423–433.
- Wall, S.C., Gu, H., and Rudnick, G. (1995). Biogenic amine flux mediated by cloned transporters stably expressed in cultured cell lines: amphetamine specificity for inhibition and efflux. *Mol. Pharmacol.* *47*, 544–550.